Minireview

L-type voltage-gated calcium channels: understanding function through structure

Ming-Chuan Wang[a], Annette Dolphin[b], Ashraf Kitmitto[a,*]

[a] *Department of Biomolecular Sciences, University of Manchester Institute of Science and Technology (UMIST), Manchester M60 1QD, UK*
[b] *Department of Pharmacology, University College London, Gower St. London WC1E 6BT, UK*

Received 4 December 2003; accepted 23 February 2004

First published online 15 March 2004

Edited by Fritz Winkler and Andreas Engel

Abstract L-type voltage-gated calcium channels (VGCCs) are multisubunit membrane proteins that regulate calcium influx into excitable cells. Within the last two years there have been four separate reports describing the structure of the skeletal muscle VGCC determined by electron microscopy and single particle analysis methods. There are some discrepancies between the structures, as well as reports for both monomeric and dimeric forms of the channel. This article considers each of the VGCC structures in terms of similarities and differences with an emphasis upon translation of data into a biological context.

Key words: L-type voltage-gated calcium channel; Single particle analysis; Electron microscopy; Angular reconstitution; Muscle excitation–contraction coupling

1. Introduction

Muscle contraction is regulated by elevation of the intracellular Ca^{2+} concentration mediated by the interplay between two membrane proteins, the L-type voltage-gated calcium channels, VGCCs, and ryanodine receptors, RyRs. Despite the involvement of the same proteins (VGCCs and RyRs), albeit tissue-specific isoforms, the molecular mechanisms governing skeletal and cardiac muscle excitation–contraction (E–C) coupling are believed to significantly differ. In skeletal muscle a direct mechanical interaction of the VGCC and the RyR (RyR1) is thought to form the basis of E–C coupling whereby upon depolarisation of the membrane the VGCC acts as a voltage sensor with conformational changes of the channel leading to a physical interaction with RyR1, promoting its opening, and triggering the release of Ca^{2+} from internal stores [1]. In contrast, depolarisation of cardiac myocytes is suggested to lead to the opening of the L-type calcium channels with Ca^{2+} influx through the VGCCs stimulating the opening of the RyR (RyR2), resulting in a cascade of Ca^{2+} ions released into the cytosol, i.e. calcium-induced calcium release, CICR [2,3]. However, there remain substantial deficiencies in the current understanding of the mechanisms involved for mediating both mechanical coupling and CICR at the molecular level.

The skeletal muscle VGCC is composed of four non-covalently associated polypeptides, the pore forming $\alpha_1$1.1 subunit, and three auxiliary subunits $\alpha_2\delta_1$, β_{1a} and γ_1 forming a heterooligomeric membrane protein, with an approximate molecular mass of 430 kDa [4]. The cardiac L-type calcium channel is assembled from three tissue-specific isoforms of α_1 ($\alpha_1$1.2), $\alpha 2\delta_1$, and β (largely the β_2 and β_3 isoforms) with no evidence as yet for a cardiac γ polypeptide. The role of the γ subunit in muscle E–C coupling is not well understood; however, from studies of γ_1 null mice it was demonstrated that though the γ_1 polypeptide is involved in modulating the current amplitude and inactivation kinetics of the channel, it is not necessary for propagating skeletal muscle E–C coupling [5]. Therefore the absence of a cardiac γ subunit in the channel assembly cannot provide a simple explanation as to the differences in mechanisms of muscle E–C coupling. The II–III intracellular loop of the $\alpha_1$1.1 polypeptide has been implicated as a major determinant for VGCC interaction with RyR1 [6], though involvement of several other 'microdomains' such as the I–II loop and regions of C-terminus have been described [7]. The molecular mechanisms governing E–C coupling are further complicated by the potential involvement of proteins such as calmodulin, calmodulin kinase II and triadin, e.g. [8–12].

2. Ultrastructure and spatial organisation of VGCC and RyR in cardiac and skeletal muscle

Some of the first glimpses into the ultrastructure and spatial organisation of both the VGCCs and RyRs came from work by Franzini-Armstrong and coworkers using freeze-fracture methods e.g. [13,14]. The VGCCs were shown to be localised to the T-tubular (T-t) membranes, invaginations of the plasma membrane, and physically separated from the RyRs residing in the junctional sarcoplasmic reticulum (jSR). Freeze-fracture replicas showed that in both skeletal and cardiac muscles VGCCs were clustered, but into different geometries with the skeletal muscle VGCCs seeming to form ordered tetrads whereas the cardiac VGCCs adopted a more random distribution. Similar studies of the RyRs in skeletal and cardiac muscle found highly ordered organisations with minor differences detectable in terms of spatial arrangement between the two tissue types.

*Corresponding author. Fax: (44)-161-2360409.
E-mail address: a.kitmitto@umist.ac.uk (A. Kitmitto).

0014-5793/04/$30.00
doi:10.1016/S0014-5793(04)00253-4

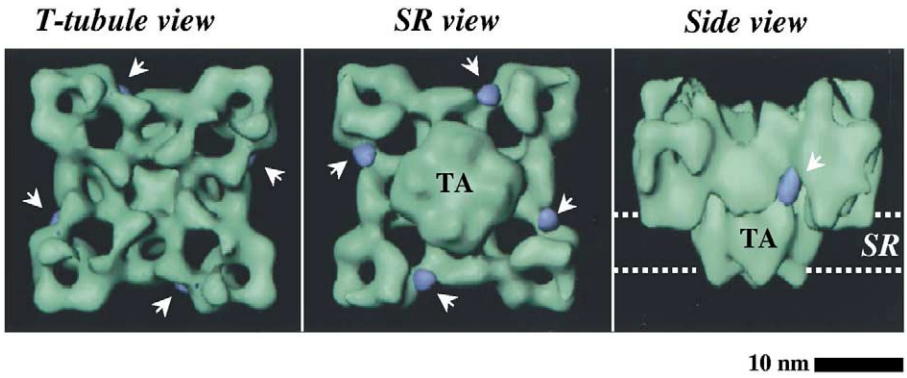

Fig. 1. 3D reconstruction of the RyR1 from rabbit skeletal muscle (adapted from Samsó et al. [29] with permission). Left panel: Cytoplasmic view, opposing the T-t membrane. Middle panel: View showing the sarcoplasmic surface illustrating the density forming the transmembrane assembly (TA). Right panel: Side view, normal to the four-fold axis. Dashed white lines indicate putative position of the jSR. The densities shaded in blue in each of the panels (indicated by the white arrows) represent the locations of bound imperatoxin A-biotin:streptavidin as determined in [28].

3. Electron microscopy (EM) and single particle analysis (SPA) methods of the RyRs

The application of EM techniques, coupled with image processing, for analysing membrane protein structures has led over the past 10 years to some significant breakthroughs from studies of two-dimensional (2D) crystals, e.g. the nicotinic acetylcholine receptor (nAchR) [15] and aquaporin [16], as well as single protein molecules, e.g. the voltage-gated sodium [17] and potassium channels [18], the skeletal muscle VGCC [19–23], and RyR [24,25]. Advantages of the single particle approach are that (i) only low microgram quantities are required for analysis, (ii) it is suitable for the study of large, multisubunit complexes, (iii) different conformational states can be captured, and (iv) it can be used for studying protein–protein (ligand) interaction (for review of SPA see [26]). It was from EM/SPA methods that the first detailed structure (~3 nm resolution) for the skeletal muscle RyR1 was first determined [24]. The RyR1 was shown to be composed of two distinct parts, a large complex cytoplasmic loosely packed structure (28×28×14 nm) attached to a smaller transmembrane domain constituting ~20% of the RyR1 mass (see Fig. 1). Following a similar strategy, the structure of the cardiac isoform (RyR2) was revealed, at a similar resolution, to have a virtually identical three-dimensional (3D) structure to RyR1 though minor differences at the edge of the cytoplasmic domain were observed [27], the significance of this is not established. Further applications of EM/SPA to investigate the structure of the RyRs include 3D mapping of proteins such as calmodulin with RyR1 [28]. In terms of understanding the interaction of the skeletal muscle VGCC with RyR1, studies using the toxin imperatoxin A ($IpTx_a$), proposed to mimic the II–III loop of $\alpha_1$1.1, have been undertaken [29] revealing that for each RyR1 tetramer four $IpTx_a$ were associated. Using difference mapping the $IpTx_a$ binding sites were localised, as illustrated in Fig. 1 (blue domains indicating the $IpTx_a$ binding sites), to the edges of the cytoplasmic assembly and located ~11 nm away from the transmembrane pore. The centre-to-centre distance between each of the $IpTx_a$ binding domains was shown to be ~15 nm.

4. Structural studies of skeletal muscle VGCC monomers and dimers

Since the VGCCs are enriched in the skeletal muscle T-t membranes (though yields remain typically less than 100 μg/400 g wet muscle tissue) studies have tended until recently [23] to concentrate upon the skeletal muscle form. Structural data for the quaternary organisation of the VGCCs have, to date, all been determined using EM/SPA methods. In 2001 Murata et al. [19] published 2D projection images (~2.7 nm resolution) of negatively stained (uranyl acetate) monomeric rabbit skeletal muscle VGCCs, revealing an asymmetric rod-like structure with a height of ~21 nm and diameter of ~10 nm with a small spherical domain, roughly 7 nm in diameter, extending from one end of the rod as shown in Fig. 2A. From a combination of antibody labelling experiments and examination of structures after removal of the $\alpha_2\delta$ subunit it was concluded that the spherical protuberance was formed by the $\alpha_2\delta$ polypeptide, and that the rod-shaped view represented the side orientation of the VGCC complex with the skeletal muscle channel spanning the T-t membrane by ~21 nm.

The following year (2002) Serysheva and coworkers presented the first 3D structure of a monomeric rabbit skeletal muscle VGCC [20] determined from frozen-hydrated protein, as shown in Fig. 2B. The 3D structure, at 3 nm resolution, was found to be comprised of two domains, termed a heart region and a handle region, tilted with respect to each other, with overall dimensions of ~11.5×13.0×12.0 nm and cavity with a radius of ~3 nm formed between the two domains. Clearly, the 3D volume in terms of height is some 7 nm shorter than the projection images presented by Murata et al. which cannot alone be accounted for by the differences in sample preparation, i.e. negative staining compared to cryo-EM methods, suggesting significant differences exist between the two structures. The heart-shaped portion of the complex was proposed to span the membrane and house the $\alpha_1$1.1, β and γ polypeptides, with the handle-shaped domain and upper portion of the heart region formed by the $\alpha_2\delta$ subunit, as depicted in Fig. 2B.

Earlier this year (2003) a further 3D structure for a mono-

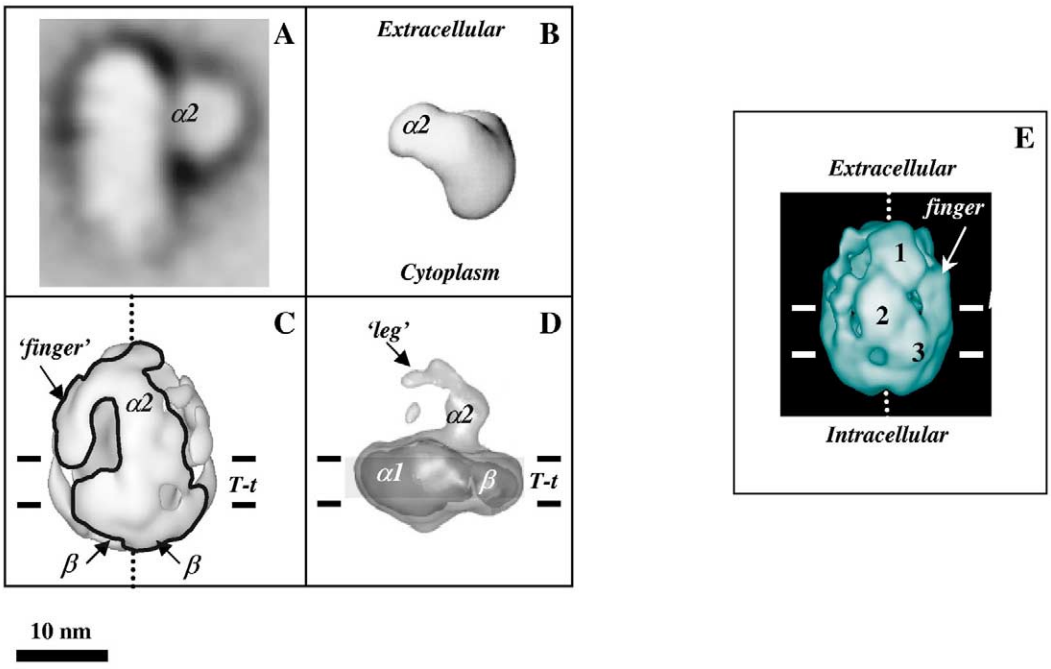

Fig. 2. Reported structures for the L-type VGCC. A: Projection image showing putative side view of a monomeric form of the skeletal muscle VGCC negatively stained (uranyl acetate) at 2.7 nm resolution, taken from Murata et al. [19] with permission. B: Putative side view of the 3D structure of the skeletal muscle VGCC (3.0 nm resolution) determined from unstained frozen-hydrated samples, displayed using surface rendering enclosing a volume corresponding to the molecular mass (~430 kDa) of a monomer taken from [20] with permission. C: Surface-rendered 3D structure (~2.5 nm resolution) of a skeletal muscle VGCC dimer embedded in trehalose/ammonium molybdate, displayed at 3σ above the mean density, to reveal the principal protein densities. The black outline illustrates the approximate contribution, at high thresholds, of the foremost monomer. The C2 symmetry axis is indicated by the dotted black vertical line. The putative position of the T-t membrane is indicated in the figure in accordance with data reported in [21,23]. D: Solid body representation of a putative side view (i.e. along the membrane plane, indicated by the shaded bar) of the 3D structure (at 2.3 nm resolution) of a monomeric skeletal muscle VGCC from unstained frozen-hydrated samples, adapted from [22] with permission. The 3D volume is displayed at two thresholds, with the light grey envelope encompassing a volume of ~550 kDa, and the higher threshold (dark grey) delineating the globular density. E: 3D structure of the cardiac L-type VGCC [31]. Side view (i.e. along the membrane plane) of the cardiac VGCC determined from negatively stained (uranyl acetate) protein purified from bovine heart displayed using surface rendering at a threshold of 1σ above the mean density. The putative position of the lipid bilayer is indicated by the white dashed lines, with the white dotted vertical line indicating the C2 symmetry axis. The principal protein densities forming the monomer arch are labelled 1–3 on the figure.

meric rabbit skeletal muscle VGCC was determined from unstained samples but at a higher resolution of ~2.3 nm (see Fig. 2D) [22]. This structure surprisingly bore little resemblance to the Serysheva volume, as can be seen by comparing Fig. 2B and D. The 3D structure showed a 'leg' domain extending out from a large globular density, measuring 16.5×14.5×8.0 nm, with the attached 'leg' having a length of ~9.5 nm. Antibody labelling with anti-β and anti-α2 IgGs led to the proposal that the leg domain formed part of the α2 protein, though it was concluded to be too small to alone accommodate the entire subunit. From the antibody labelling data the 3D structure was orientated with respect to the T-t membrane as shown in Fig. 2D, placing the globular domain within the bilayer, with the leg extending on the extracellular side. Therefore the major protein density is residing within the membrane as opposed to the models proposed by Murata et al. [19] and Serysheva et al. [20] in which the rod- and heart-shaped structures (respective equivalents to the globular domain), span the membrane with an asymmetric distribution of the protein mass across the membrane.

We have also reported a 3D structure, at 2.7 nm resolution, for the skeletal muscle (rabbit) VGCC but of a dimeric form of the complex [21]. The 3D structure was determined from negatively stained (uranyl acetate) purified skeletal muscle VGCC, using the random conical tilt technique [30]. This structure has recently been refined after embedding the purified channel in trehalose/ammonium molybdate [23], with a 3D reconstruction performed using the angular reconstitution method [31], to a resolution of 2.5 nm. The two structures derived using different negative stains and reconstructive methods generated very similar 3D volumes as described in [23]. In both studies the skeletal muscle dimer was found to be formed by two arch-shaped monomers 22–23 nm in height and ~8 nm thick, with contacts at the tips of the arches leading to the formation of a central aqueous cavity roughly 7 nm in diameter. Two finger-like protrusions, extending out from the arches, coil around on each side and isolate the central chamber from the external environment. Antibody (anti-β) and lectin gold labelling permitted orientation of the skeletal muscle dimer with respect to the T-t membrane [23] as depicted in Fig. 2C. Moreover, by using negative staining techniques it was possible to determine that the cavity was not entirely sealed off from the extracellular milieu with the stain found to penetrate through to the interior via a series of small holes perforating the outer surface of the finger domains.

On examination of the preparative methods leading to the monomeric and dimeric forms it can be found that one of the principal differences lie with the detergent used for channel solubilisation. For purification of the VGCC dimers CHAPS

was used as the solubilising agent, with exogenous lipid (asolecithin) added to all buffers throughout the purification (detergent:lipid ratio of 2:1) whereas digitonin was employed for the isolation of the monomeric form in [19,20,22]. Interestingly, rotary shadowed images of freeze-dried, purified rabbit skeletal muscle VGCC complexes using CHAPS/asolecithin in the Campbell laboratory [32] showed channel complexes with very similar dimensions and gross structural features to the dimers reported in [21,23]. Dissociation of the VGCC dimers showed monomeric complexes [23] that could be associated with various orientations of the 3D structure presented by Wolf [22] and projection images in [19].

5. Comparison of the monomeric and dimeric skeletal muscle VGCC structures

Examination of the structures shown in Fig. 2A, B and D [19,20,22] finds significant differences between the structures proposed for a monomeric skeletal muscle VGCC that cannot alone be attributed to either the use of negative staining or cryo-EM techniques, since both of the 3D structures (B and D) were determined from unstained frozen-hydrated specimens. In addition, both 3D studies employed the angular reconstitution method [33,34], though different software was utilised for each reconstruction. The 3D structure reported in [22] (Fig. 2D) is at a higher resolution than that presented in [20] (Fig. 2B) and is therefore inevitably more detailed; but whether the same structure at 3 nm resolution would show similar features to that in [20] is unclear.

The 3D dimer structure shown in Fig. 2C is displayed at a threshold (3σ above the mean density) to display the principal structural features. The monomer arches show a clear similarity in terms of overall dimensions to the rod-shaped structures reported by Murata and coworkers [19], with a finger density correlating to the protruding spherical domain, as highlighted in the figure by the black outline indicating the approximate boundaries of the foremost monomer. Though it is hard to equate the dimeric structure to the Serysheva model in [20] there are features common to the monomeric 3D structure presented by Wolf and coworkers [22]. For example, the monomer 'leg domain' can be matched to one of the dimer fingers, suggested in both reports to be formed by the α_2 polypeptide, with the globular domain of the monomer corresponding to a monomer arch in the dimer. The length of the globular domain in [22] is slightly shorter than the height of the monomer arch in [21,23] and this discrepancy may be explained, in part, by a different detergent annulus and the use of negative stains for studies of the dimeric structure. However, correlation of the two structures in this manner may open the way for an alternative interpretation of the monomer structure orientation with respect to the T-t membrane with rotation of the structure as shown in Fig. 2D by 90° counterclockwise so that the globular domain spans the membrane. With the monomeric VGCC placed within the T-t membrane as shown in Fig. 2D the β polypeptide is localised to the lipid bilayer. It is well established that the β polypeptide is hydrophilic [35] and is shown by many functional and other studies to be localised to the periphery of the membrane boundary on the intracellular side of the membrane. Therefore, an advantage of the reorientation of the monomeric 3D volume of Wolf et al. [22], so that the globular domain traverses the bilayer, is that the β subunit would be placed within the cytosol and not embedded within the T-t membrane.

6. Structural studies of the cardiac VGCC

We have recently purified the cardiac VGCC from bovine heart. Intriguingly, both stable monomeric and dimeric forms were isolated using digitonin for solubilisation, as discussed in [23]. Comparison of the skeletal and cardiac VGCC dimer structures revealed a common architectural design. This is particularly apparent when the cardiac 3D volume is viewed in a similar orientation to the skeletal muscle dimer (Fig. 2C) as shown in Fig. 2E, with the monomer arch and associated finger domains clearly apparent. The backbone of the cardiac monomer arch is kinked in the middle compared to that in the skeletal muscle structure (Fig. 2C) and is resolved into three protein densities numbered 1–3 on the figure. Differences between the two structures in the region tentatively assigned to the transmembrane domain as reported in [23] were identified with a tapering of the cardiac VGCC structure compared to the skeletal muscle form. This finding was in keeping with the concept of the cardiac channel composition lacking the γ subunit, proposed to be an integral membrane polypeptide [36]. In addition, the overall dimensions of the cardiac VGCC were found to be slightly smaller than the skeletal muscle counterpart, with a height of $\sim$19 nm and a width of $\sim$14.5 nm.

7. Oligomeric forms of the VGCCs and RyRs

Physiologically functional oligomeric forms of integral membrane proteins are not unusual, for example the RyR exists as a homotetramer as described, as does the type 1 inositol 1,4,5-trisphosphate receptor [37,38]. However, when purifying proteins using detergents, detergent-induced oligomerisation can occur and therefore isolation of an oligomeric form does not necessarily represent the functional unit. The finding that both the skeletal and cardiac muscle VGCCs can be isolated as dimers, formed by a head-to-head association and thus in principle having the potential to be physiologically viable, is nevertheless intriguing. Although the concept of functional dimeric VGCCs appears to be novel, data from other types of experiments can be found that lend support to the possibility of a functional oligomeric form. For example, Hymel et al. [39] reported that upon functional reconstitution of purified skeletal muscle VGCC their data could only be explained by the association of the VGCCs into larger oligomeric functional complexes. It has also proven extremely difficult to express the $\alpha_1$1.1 polypeptide in heterologous systems and this may also pertain to the dimeric structure. Of possible relevance for both geometric and stoichiometric association of VGCCs and RyRs is the finding by Marks and coworkers that RyR tetramers (RyR1 and RyR2) when reconstituted into proteoliposomes formed oligomers of tetramers that were functional, with the channels gating simultaneously [40]. Previous modelling of the VGCC dimer with RyR1 as described in [21] found that the VGCC putative interaction sites with RyR1 correlated roughly to the spacing of the $IpTx_a$ binding sites [29]. In a similar manner we present here (Fig. 3) a possible configuration of the skeletal muscle VGCC dimer (refined structure recently reported in [23]) and RyR1 complex. Illustrated in Fig. 3A is a potential arrange-

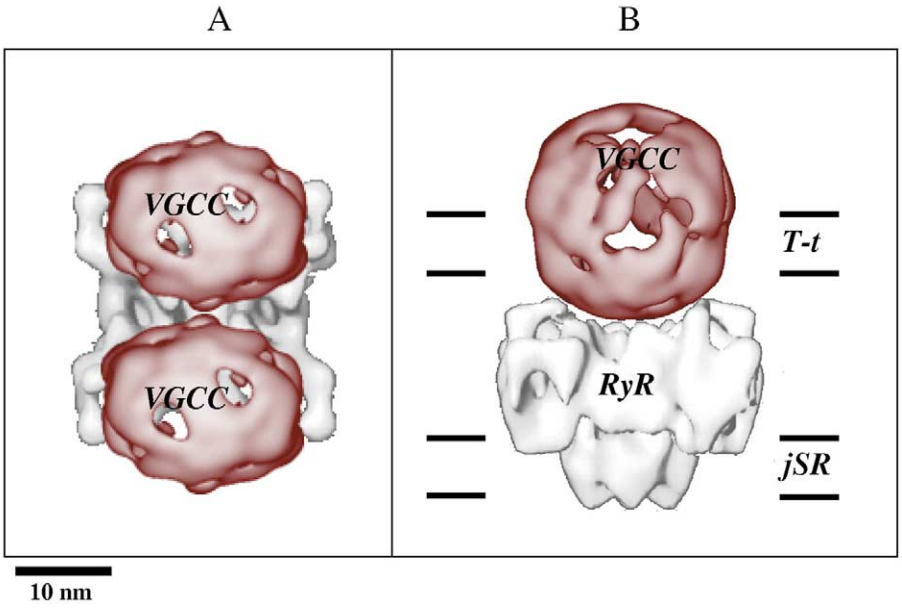

Fig. 3. Model depicting putative interaction sites of two skeletal muscle VGCC dimers with a RyR1 tetramer. A: Two VGCC dimers (surface rendered and displayed at 2.5σ above the mean density) superimposed on the RyR extracellular face with respect to the jSR (adapted from [29]). B: Side view (parallel to the membrane plane) of the VGCC–RyR1 complex.

ment of two VGCC dimers superimposed onto the face of the RyR1 tetramer that extends towards the T-t membrane. Shown in Fig. 3B is a side view (parallel to the membrane plane) of a VGCC–RyR1 complex.

8. Conclusions

Whether the monomeric, dimeric or higher oligomeric forms of the skeletal or cardiac VGCC represent functional units remains to be established. How the observation of oligomeric forms of both the VGCCs and RyR tetramers can be equated to freeze-fracture studies (e.g. [13]) is not yet clear, though it is now imperative to establish whether oligomeric units play a functional role in vivo, and if so, to establish whether oligomer formation is one of the determinants that dictates a mechanical interaction mechanism or CICR mode of E–C coupling. The obvious differences between the structures described in Fig. 2 illustrate that structural studies of VGCCs are less well developed than for example the RyR. However, there are also common elements, with a consensus that the extracellular α2 polypeptide (an ~140 kDa glycoprotein, with its functional role not fully resolved) is a domain extending out from a large rod- (Murata), heart- (Serysheva), globular (Wolf), or arch- (Wang) shaped density. For translation of structural data to physiological function a priority will be to extend the resolution of the structures to identify subunit boundaries with more precise labelling studies (e.g. Fab fragments) and to also examine interchannel VGCC–RyR crosstalk. EM coupled with SPA methods presents an ideal approach to examine whole protein–protein interactions, with restrictive yields, and for a RyR–VGCC complex that may equate to a macromolecular assembly with a molecular mass in excess of 4 MDa.

Acknowledgements: A.K. holds a British Heart Foundation Basic Science Lectureship Award, BS/97002.

References

[1] Rios, E. and Brum, G. (1987) Nature 325, 717–720.
[2] Cheng, H., Cannell, M.B. and Lederer, W.J. (1994) Pflugers Arch. Eur. J. Physiol. 428, 415–417.
[3] Santana, L.F., Cheng, H., Gomez, A.M., Cannell, M.B. and Lederer, W.J. (1996) Circ. Res. 78, 166–171.
[4] Leung, A.T., Imagawa, T. and Campbell, K.P. (1987) J. Biol. Chem. 262, 7943–7946.
[5] Arikkath, J., Chen, C.C., Ahern, C., Allamand, V., Flanagan, J.D., Coronado, R., Gregg, R.G. and Campbell, K.P. (2003) J. Biol. Chem. 278, 1212–1219.
[6] Nakai, J., Tanabe, T., Konno, T., Adams, B. and Beam, K.G. (1998) J. Biol. Chem. 273, 24983–24986.
[7] Tanabe, T., Beam, K.G., Adams, B.A., Niidome, T. and Numa, S. (1990) Nature 346, 567–569.
[8] Yang, D.M. et al. (2003) Circ. Res. 92, 659–667.
[9] Wu, Y.J., Colbran, R.J. and Anderson, M.E. (2001) Proc. Natl. Acad. Sci. USA 98, 2877–2881.
[10] Meissner, G. and Lu, X.Y. (1995) Biosci. Rep. 15, 399–408.
[11] Guo, W., Jorgensen, A.O. and Campbell, K.P. (1994) J. Biol. Chem. 269, 28359–28365.
[12] Tang, W., Sencer, S. and Hamilton, S.L. (2002) Front. Biosci. 7, D1583–D1589.
[13] Block, B.A., Imagawa, T., Campbell, K.P. and Franzini-Armstrong, C. (1988) J. Cell Biol. 107, 2587–2600.
[14] Franzini-Armstrong, C. and Jorgensen, A.O. (1994) Annu. Rev. Physiol. 56, 509–534.
[15] Miyazawa, A., Fujiyoshi, Y., Stowell, M. and Unwin, N. (1999) J. Mol. Biol. 288, 765–786.
[16] Walz, T. et al. (1997) Nature 387, 624–627.
[17] Sato, C., Ueno, Y., Asai, K., Takahashi, K., Sato, M., Engel, A. and Fujiyoshi, Y. (2001) Nature 409, 1047–1051.
[18] Sokolova, O., Kolmakova-Partensky, L. and Grigorieff, N. (2001) Structure 9, 215–220.
[19] Murata, K., Odahara, N., Kuniyasu, A., Sato, Y., Nakayama, H. and Nagayama, K. (2001) Biochem. Biophys. Res. Commun. 282, 284–291.
[20] Serysheva, I.I., Ludtke, S.J., Baker, M.R., Chiu, W. and Hamilton, S.L. (2002) Proc. Natl. Acad. Sci. USA 99, 10370–10375.
[21] Wang, M.-C., Velarde, G., Ford, R.C., Berrow, N.S., Dolphin, A.C. and Kitmitto, A. (2002) J. Mol. Biol. 323, 85–98.

[22] Wolf, M., Eberhart, A., Glossmann, H., Striessnig, J. and Grigorieff, N. (2003) J. Mol. Biol. 332, 171–182.
[23] Wang, M.-C., Collins, R.C., Ford, R.C., Berrow, N., Dolphin, A.C. and Kitmitto, A. (2004) J. Biol. Chem. 279, 7159–7168.
[24] Radermacher, M., Rao, V., Grassucci, R., Frank, J., Timerman, A.P., Fleischer, S. and Wagenknecht, T. (1994) J. Cell Biol. 127, 411–423.
[25] Baker, M.L., Serysheva, I.I., Sencer, S., Wu, Y.L., Ludtke, S.J., Jiang, W., Hamilton, S.L. and Chiu, W. (2002) Proc. Natl. Acad. Sci. USA 99, 12155–12160.
[26] Ruprecht, J. and Nield, J. (2001) Prog. Biophys. Mol. Biol. 75, 121–164.
[27] Sharma, M.R., Penczek, P., Grassucci, R., Xin, H.B., Fleischer, S. and Wagenknecht, T. (1998) J. Biol. Chem. 273, 18429–18434.
[28] Samso, M. and Wagenknecht, T. (2002) J. Biol. Chem. 277, 1349–1353.
[29] Samso, M., Trujillo, R., Gurrola, G.B., Valdivia, H.H. and Wagenknecht, T. (1999) J. Cell Biol. 146, 493–499.
[30] Frank, J., Radermacher, M., Penczek, P., Zhu, J., Li, Y.H., Ladjadj, M. and Leith, A. (1996) J. Struct. Biol. 116, 190–199.
[31] Ludtke, S.J., Baldwin, P.R. and Chiu, W. (1999) J. Struct. Biol. 128, 82–97.
[32] Leung, A.T., Imagawa, T., Block, B., Franzini-Armstrong, C. and Campbell, K.P. (1988) J. Biol. Chem. 263, 994–1001.
[33] Vanheel, M. (1987) Ultramicroscopy 21, 111–123.
[34] Serysheva, I.I., Orlova, E.V., Chiu, W., Sherman, M.B., Hamilton, S.L. and Vanheel, M. (1995) Nat. Struct. Biol. 2, 18–24.
[35] Walker, D. and De Waard, M. (1998) Trends Neurosci. 21, 148–154.
[36] Jay, S.D., Ellis, S.B., McCue, A.F., Williams, M.E., Vedvick, T.S., Harpold, M.M. and Campbell, K.P. (1990) Science 248, 490–492.
[37] Serysheva, I.I., Bare, D.J., Ludtke, S.J., Kettlun, C.S., Chiu, W. and Mignery, G.A. (2003) J. Biol. Chem. 278, 21319–21322.
[38] Jiang, Q.X., Thrower, E.C., Chester, D.W., Ehrlich, B.E. and Sigworth, F.J. (2002) EMBO J. 21, 3575–3581.
[39] Hymel, L., Striessnig, J., Glossmann, H. and Schindler, H. (1988) Proc. Natl. Acad. Sci. USA 85, 4290–4294.
[40] Marks, A.R., Marx, S.O. and Reiken, S. (2002) Trends Cardiovasc. Med. 12, 166–170.